INTERNATIONAL JOURNAL OF INTEGRATED ENGINEERING
ISSN: 2229-838X e-ISSN: 2600-7916

IJIE

Vol. 17 No. 2 (2025) 315-325
https://publisher.uthm.edu.my/ojs/index.php/ijie

Image Pre-processing and Quality Analysis Using Structural Similarity Indexing for Drone Applications

Muhammad Nuh Shamsudin[1], Suhaili Beeran Kutty[2]*, Puteri Nor Ashikin Megat Yunus[3], Asyraf Ahmad Safri[4], Mohamad Ad-Fadhil Musa[5]

[1] *Rankine & Hill Sdn Bhd, Unit 02-13, Blok H, Komersial Southkey Mozek, Persiaran Southkey 1, Kota Southkey, 80150 Johor Bahru, Johor, MALAYSIA*
[2] *Faculty of Electrical Engineering, Universiti Teknologi MARA (UiTM) Johor Branch, Pasir Gudang Campus, Bandar Seri Alam, 81750 Masai, Johor, MALAYSIA*
[3] *Faculty of Electrical Engineering, Universiti Teknologi MARA, 40450 Shah Alam, Selangor, MALAYSIA*
[4] *ATSE Solutions Sdn Bhd, B-4-1, Ostia Bangi Business Avenue, Seksyen 14, 43650 Bandar Baru Bangi, Selangor, MALAYSIA*
[5] *Standard Encoder (Malaysia) Sdn Bhd, 3, Jalan Kempas 5/5, Kawasan Perindustrian Kempas, 81200 Johor Bahru, Johor, MALAYSIA*

*Corresponding Author: suhaili88@uitm.edu.my
DOI: https://doi.org/10.30880/ijie.2025.17.02.026

Article Info

Received: 28 March 2025
Accepted: 23 July 2025
Available online: 8 August 2025

Keywords

Image quality assessment, SSIM, drone, gaussian filtering, median filtering, solar panel inspection

Abstract

The increasing popularity of drones in mapping, surveying, and inspection processes underscores their potential in various industrial applications. Despite their widespread use, the accuracy and reliability of drone imagery for solar panel inspection have not been extensively verified. This paper introduces a novel image quality assessment method for drone applications, utilizing the Structural Similarity Indexing Method (SSIM). The proposed methodology evaluates the quality of images captured by drones, focusing on the drone's positional relationship to the solar panels under diverse conditions. The study compared the quality of images with those subjected to Gaussian and Median filtering. The SSIM was employed as the primary metric to quantify the similarity between the original and processed images, providing a robust measure of image quality degradation or enhancement. In indoor tests, the SSIM values consistently decrease as the height increases from 0.7m to 2.5m for both Median and Gaussian filters. Meanwhile, outdoor tests reveal that the image achieves its highest SSIM score at a height of 1.0m for both Median and Gaussian filters. It is important to note that the Gaussian filter consistently yields slightly higher SSIM values compared to the Median filter at all heights. The SSIM analysis revealed significant insights into the optimal conditions for drone imaging in solar panel inspections. The findings of this research contribute to the development of standardized practices for drone-based inspections, ensuring high accuracy and reliability.

1. Introduction

Image Quality Assessment (IQA) is the process of evaluating the quality of an image using various methods and metrics, aiming to quantify the visual quality of an image in a manner that correlates with human perception [1].

IQA is critical in various applications, such as image processing, computer vision, multimedia, and photography, where maintaining or improving image quality is essential. The most common metrics used to validate the IQA are the Peak Signal-to-Noise Ratio (PSNR), Mean Squared Error (MSE), and Structural Similarity Indexing Method (SSIM).

The SSIM approach evaluates the similarity of two images by comparing structural data from each image, including luminance, contrast, and structure of the image. The finding values range from -1 to 1, with higher values indicating greater similarity and, hence, better quality [2]. SSIM is generally considered a better-quality metric than PSNR and MSE [3]. SSIM compares local patterns of pixel intensities normalized for luminance and contrast, which closely aligns with how humans perceive visual information. A drawback of SSIM was its inaccuracy when assessing blurry images. However, improvements have enhanced SSIM's capability to handle blurry images effectively [4].

Drones have become increasingly popular for image acquisition due to their ability to access hard-to-reach areas and their cost-effectiveness compared to traditional aerial imaging methods [5]. Weather, wind, and lighting conditions can complicate aerial image capture, leading to noise, color distortion, or darker images, which may degrade the overall image quality [6]. IQA is an important step in the image acquisition process for drones as it ensures that the images captured are of high quality and suitable for their intended use in mapping, surveying, and inspection. IQA also helps to identify and correct any issues with the images. Images taken by drones, also known as unprocessed or uncompressed images, are influenced by several factors related to the drone's imaging system, environmental conditions, and the intended application of the images [7].

Drones are increasingly used for inspecting solar farms due to their efficiency, safety, and ability to capture detailed data [8]. From the image of the solar panel, many different defects could be detected, such as cracks and degradation of the quality of the panel [9]. However, there are some problems with using aerial photography or drones to capture the image of the target, as it is difficult to determine the best position and location of the drone in capturing the images of the PV plant [10–11]. Many factors affect the movement and steadiness of the drone during image capturing, such as weather and location. Therefore, the quality of the images will be affected too.

A study by Tian et al. [12] lists three different flight heights, which are 80m, 150m, and 200m flight, and one of the metrics to validate the result is a signal-to-noise ratio. Next, Lim et al. [13] assess image quality after being taken by a drone by evaluating the image's National Image Interpretability Rating Scale (NIIRS). Their work shows that the lower the altitude of an image, the higher the image quality is produced, but there is a certain threshold for the lower altitude [13]. A study in 2023, [14] shows the altitude to get better-quality drone capture an image is below 100m. Another study related to image quality assessment was conducted by Dąbrowski and Jenerowicz [15]. They assess the image quality produced by different sensors equipped with the drone [15]. The image quality will then be observed based on the drone's height relative to the images and three parameters: spatial, spectral, and radiometric. Work on drone imaging quality has also been done by Benjak and Hofman [16] where video capturing is analysed to determine compression efficiency.

The image quality of the PV images captured by drones from various positions and angles for inspection needs to be analysed. The analysis is important because the most favourable drone heights and positions that yield the highest image quality could be identified, which is crucial for effective solar panel inspection [17–18]. This paper aims to analyse the image quality based on the drone's height relative to the solar panel under various conditions using the SSIM metric.

2. Methodology

In this study, image quality analysis was carried out by creating a photography plan, acquiring images with drones, image filtering, and examining the SSIM of the acquired image.

2.1 Photographing Plan & Camera Specification

In this preliminary stage, the location of the experiment, the method to acquire the image, and the subject to be shot are determined. The locations are a close hall in the College of Engineering, Universiti Teknologi MARA (UiTM), the UiTM's hockey field, and an empty parking field at UiTM. The close hall was chosen because it is the control experiment with the low attraction of wind and environmental conditions. Two other locations were chosen to eliminate other unwanted objects in the surrounding area, with the two locations being wide and spacious. The drone's specifications, which are equipped with the camera used throughout the experiment, are shown in Table 1 and Table 2. Drone control and flying practice were done to avoid mishaps during the experiment.

Int. Journal of Integrated Engineering Vol. 17 No. 2 (2025) p. 315-325

Table 1 *Drone specification for DJI Air 2S*

Brand	DJI Air 2S
Type	Quadcopter
Weight	595g
Flight Time	30 minutes
Max Speed	19 m/s
Max Alt.	200 meters
Size	302 mm
Battery	3S, 3750mAh
Focal Length	20mm
Aperture	f/2.8
Sensor Width	25.4 mm

Table 2 *Drone specification for DJI Air 2S*

ISO	200
Focal Length	8 mm
Aperture	f/2.8
Exposure Time	1/1000~1/1500

2.2 Image Acquisition

The indoor and outdoor tests were conducted, with the object of the test being a 650 mm x 450 mm solar panel. The panel is lying down on the ground level, as shown in Fig. 1. The drone's camera is set to face the ground at a 90º angle and hovers over the center of the PV panel. Both indoor and outdoor tests capture the solar panel from heights up to 2.5m in intervals of 0.1m, starting at 0.7m. The height range of 0.7m to 2.5m is chosen to ensure optimal image quality while also accommodating a realistic spectrum of altitudes for drone operations. This selection enables investigation of the effect of altitude on image quality. It not only aligns with the theoretical limits highlighted in prior research but also fits within the practical constraints encountered in drone applications.

For morning, evening, and post-rain tests, we capture images of the subject ten times at a height of 1m to minimize the effects of random environmental factors such as wind and minor drone instability. This approach ensures reliable image quality assessment and allows for robust statistical analysis. These tests are conducted for four days, with images taken twice daily at 10 AM and 4 PM.

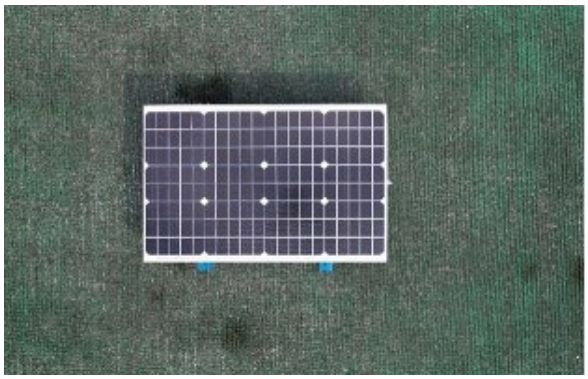

Fig. 1 *Solar panel 650 x 450mm lying on the ground level*

2.3 Image Filtering

Image filtering is a technique used in image processing to enhance or modify an image by manipulating pixel values [19]. Filtering includes reducing noise, enhancing edges, blurring, sharpening, or extracting specific features from the image. This process typically involves applying a mathematical operation to each pixel and its

neighboring pixels, which can be done using various filters. In this experiment, a median filter and a Gaussian filter were used.

The median filter is particularly useful in digital image processing for its ability to remove noise while preserving edges. It is a popular choice for applications requiring noise reduction without blurring sharp features in an image. The median filter is a non-linear image processing introduced by Tukey in 1974. The median filter will replace each pixel in an image with a mean value of the surrounding target sample.

The Gaussian filter is a smoothing filter commonly used in image processing to reduce noise and other unwanted variations in an image. It works by convolving an image with a Gaussian function, which has the effect of blurring the image while preserving its edges. The filter can be adjusted by changing the standard deviation of the Gaussian function, which controls the amount of blurring. Gaussian filters are known for their ability to preserve the edge information while smoothing out the noise.

2.4 Image Quality Analysis

SSIM is calculated by comparing the original or reference image to the compressed image that has been processed. One thing to note is that the original image must have the exact resolution as the filtered image, as the SSIM tests the structural composition between the two images. Based on Fig. 2, adapted from Uhrina et al. [20], the signal x references the original image while signal y references the filtered image. It will then go through several parameter measurements before being compared to the quality.

This research uses SSIM to determine the quality of drone images, especially in fields such as fault detection on photovoltaic (PV) panels. SSIM is well-known among various image quality measurements due to its uncomplicated principles and low computational complexity [21]. It is also a method where the image is assessed to imitate human visual perception with high subjective accuracy [22]. It is an objective quality assessment parameter to measure the similarity between two images. The luminance, contrast, and structural information in an image are all considered by SSIM to produce a score between -1 and 1, where 1 denotes a perfect match between the two images and -1 denotes no similarity.

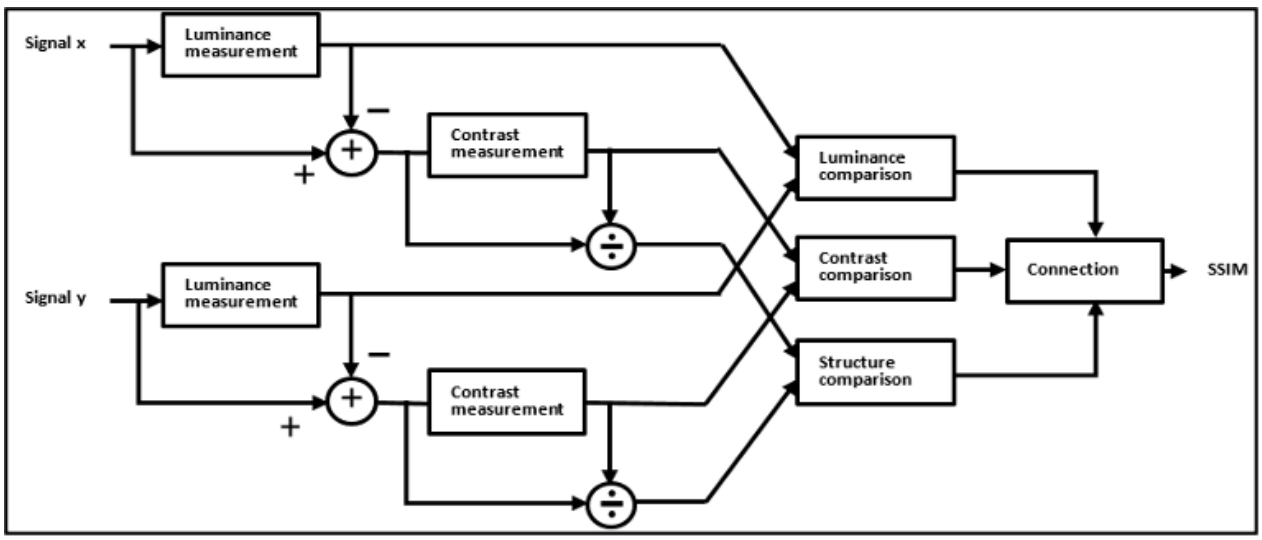

Fig. 2 *The block diagram of SSIM metric [20]*

Luminance model definition as stated in Equation (1), where μx and μy is the signal x and y mean value:

$$l(x,y) = \frac{2\mu_x\mu_y}{\mu^2{}_x + \mu^2{}_y} \tag{1}$$

Contrast model definition is shown in Equation (2), where σx and σy are the variance of images x and y:

$$c(x,y) = \frac{2\sigma_x\sigma_y}{\sigma^2{}_x + \sigma^2{}_y} \tag{2}$$

Structural model definition is shown in Equation (3), where σxy is the covariance of image x and y.

$$s(x,y) = \frac{\sigma_{xy}}{\sigma_x + \sigma_y} \tag{3}$$

When Equations (1), (2), and (3) are combined, the SSIM Equation expressed in (4) will be produced.

$$SSIM(x,y) = [l(x,y)]^{\alpha} \cdot [c(x,y)]^{\beta} \cdot [s(x,y)]^{\gamma} \tag{4}$$

The parameter from Equation (4) must be α>0, β>0, γ>0. These parameters are equal to 1. This will produce a specific form of SSIM as shown in Equation (5).

$$SSIM(x,y) = \frac{(2\mu_x\mu_y)(2\sigma_{xy})}{(\mu^2{}_x + \mu^2{}_y)(\sigma^2{}_x + \sigma^2{}_y)} \tag{5}$$

If the SSIM value is higher, it indicates a higher similarity in image x (original image) with image y (compressed image).

3. Results and Discussion

Fig. 3 shows the first and last images of the drone captured based on the height for indoor and outdoor tests. Table 3 lists the readings of each image that are applied with the Median and Gaussian filters during the indoor and outdoor tests.

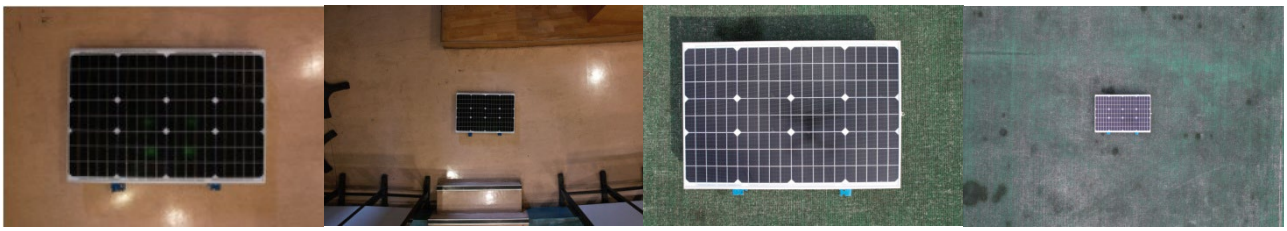

(a) **(b)** **(c)** **(d)**

Fig. 3 *(a) The solar panel's image was taken at 0.7 m in a closed hall; (b) The image was taken at 2.5m in a closed hall; (c) The image was taken at 0.7m for the outdoor test; (d) The image was taken at 2.5m for the outdoor test*

Table 3 *SSIM for indoor and outdoor tests with image filtering*

Height (cm)	Indoor Test		Outdoor Test	
	SSIM with Median Filter	SSIM with Gaussian Filter	SSIM with Median Filter	SSIM with Gaussian Filter
70	0.68473	0.70648	0.06594	0.07479
80	0.66700	0.68915	0.07959	0.08689
90	0.62230	0.64831	0.08523	0.09233
100	0.62703	0.65102	0.09341	0.09994
110	0.60940	0.63198	0.06369	0.07304
120	0.59601	0.61925	0.06295	0.07273
150	0.55562	0.57883	0.06759	0.07797
170	0.57030	0.59238	0.07414	0.08474
190	0.53540	0.55540	0.07757	0.08870
210	0.51744	0.53743	0.07637	0.08865
230	0.49591	0.51583	0.07924	0.09161
250	0.47842	0.49835	0.08027	0.09329

For indoor tests, the SSIM values decrease as the height increases from 0.7m to 2.5m for both Median and Gaussian filters. The result shows that the lowest height has the highest SSIM score. There is a slight decrease in the score at 0.9m, but it eventually gently increases back to 1.0m. On 1.7m, the score rose slightly before steadily decreasing at the next height until 2.5m, as shown in Fig. 4. These are the values when the external factors are being eliminated: the wind and the sunlight. The highest SSIM value, 0.70648, is observed at 70 cm with a Gaussian filter, and the lowest, 0.47842, at 250 cm with the Median filter. The Gaussian filter consistently produces slightly higher SSIM values compared to the Median filter at all heights. For the outdoor test, the SSIM score proves that at a height of 1.0m, the image has the highest value for both Median and Gaussian filters, which are 0.0934 and 0.09994. There is a rapid decrease of 1.1m, but it gradually increases to 2.5m. SSIM values are significantly higher indoors compared to outdoors for both filters.

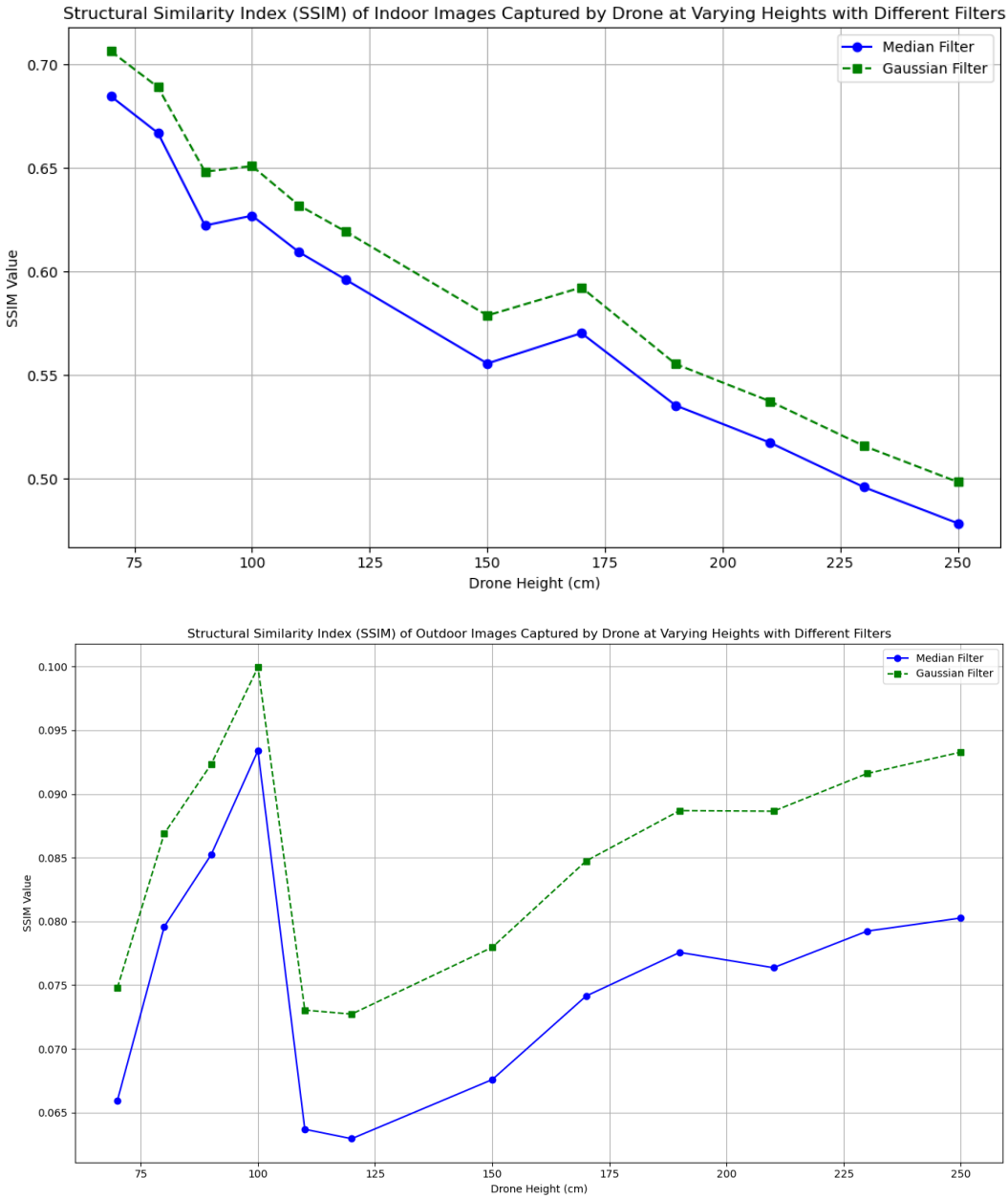

Fig. 4 *The graph of SSIM value for images in the indoor and outdoor environment*

Following the results in indoor and outdoor tests, a height of 1.0m is chosen as the fixed height used for the AM & PM and after-rain tests. For the AM & PM test, on day 1 and day 4, the test is done at the UiTM hockey field, while on day 2 and day 3, the test is done at an empty parking lot. The image samples taken are shown in Fig. 5, and the SSIM values recorded are listed in Table 4. For images with a Median filter, the SSIM value is slightly higher in the AM than the PM on day 1. Similarly, the SSIM value is higher in the AM than the PM for images with Gaussian

Int. Journal of Integrated Engineering Vol. 17 No. 2 (2025) p. 315-325

filters. For day 4, which is the same place as day 1, the SSIM values are almost equal in the AM and PM. However, for days 2 and 3, where the place is an empty parking field, the SSIM value is higher in the PM than in the AM for both filters. Based on the findings, the SSIM values for AM and PM are quite close and do not show a strong trend favoring either AM or PM. Regarding filter comparison, the Gaussian and median filters perform almost equally well.

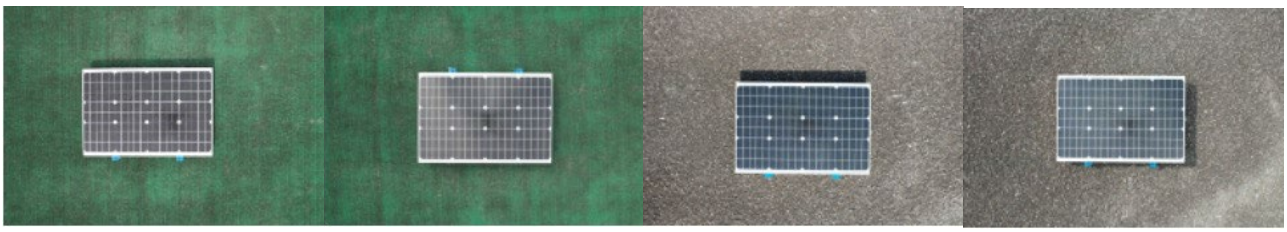

(a) **(b)** **(c)** **(d)**

Fig. 5 *Image taken from hockey field and empty parking field at 1.0m where (a) and (c) in AM and (b) and (d) in PM of the day*

Table 4 *The average of the SSIM for the AM & PM tests where solar panel is captured 10 times at a height of 1m*

Place	Day	SSIM with Median		SSIM with Gaussian	
		AM	PM	AM	PM
Hockey field	1	0.2807	0.2684	0.2776	0.2645
Empty parking field	2	0.2673	0.2769	0.2712	0.2793
Empty parking field	3	0.2710	0.2769	0.2745	0.2794
Hockey field	4	0.2700	0.2704	0.2654	0.2658

Fig. 6 shows the samples of images taken for the after-rain test stimulation, and Table 5 lists the readings of the SSIM values. The median and Gaussian filters perform better in the AM than the PM across all four days. The Gaussian filter consistently shows slightly higher SSIM values than the median filter. The bar chart in Fig. 7 visualizes the SSIM scores for drone-captured images of solar panels using different filters, which are Median and Gaussian, during AM and PM sessions at two locations over four days.

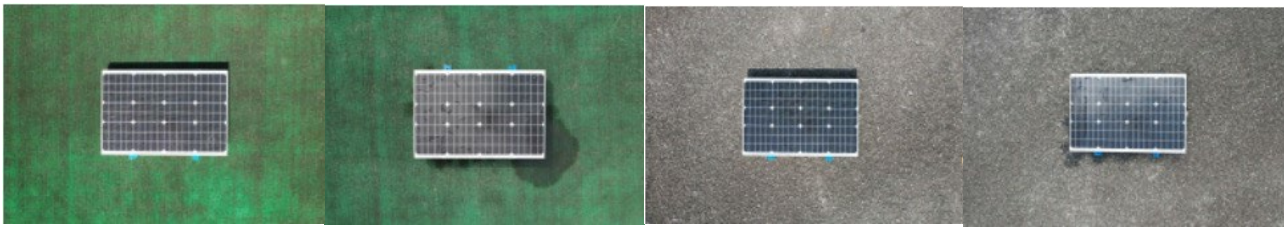

(a) **(b)** **(c)** **(d)**

Fig. 6 *Image taken from hockey field and empty parking field with after rain simulation where (a) and (c) in AM and (b) and (d) in PM of the day*

Table 5 *The SSIM for the after-rain simulation tests where the solar panel is captured 10 times at the height of 1m*

Place	Day	SSIM with Median		SSIM with Gaussian	
		AM	PM	AM	PM
Hockey field	1	0.2630	0.2165	0.2649	0.2172
Empty parking field	2	0.2753	0.2753	0.2802	0.2829
Empty parking field	3	0.2726	0.2740	0.2763	0.2778
Hockey field	4	0.2649	0.2174	0.2697	0.2328

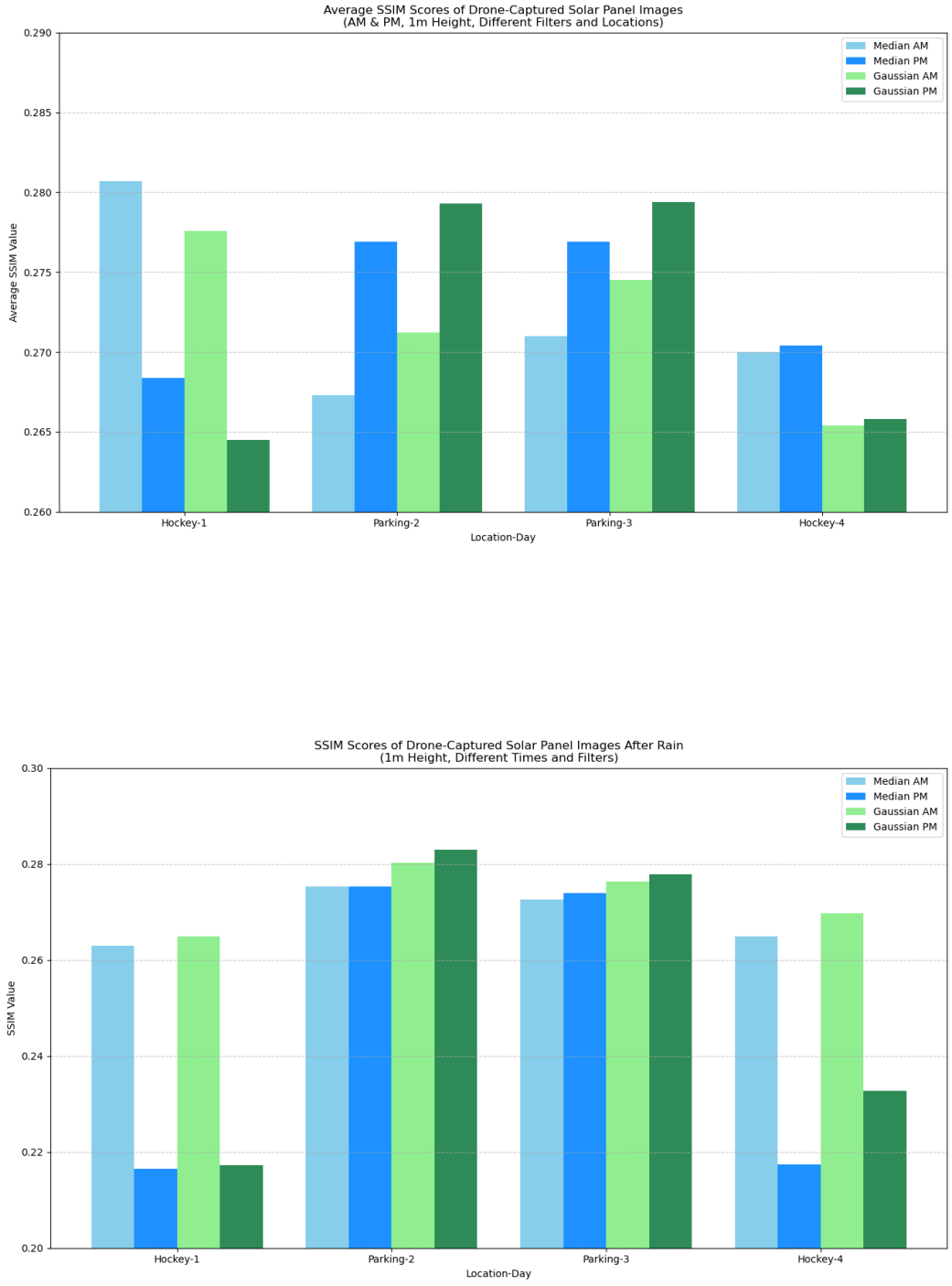

Fig. 7 *The graph shows an average of the SSIM value for images in the outdoor environment*

From the data and analysis, for the indoor experiment, it was observed that the SSIM value decreases as the drone's height increases. This could be because the SSIM assesses factors such as image brightness, contrast, and structural similarities. As the drone moves further from the target, the loss of structural detail due to increased distance may contribute to the gradual reduction in SSIM.

When capturing images with a drone in outdoor settings, it's important to consider the impact of various external factors such as natural lighting conditions, weather variables like rain or fog, and the influence of wind. These elements can significantly affect the overall quality and clarity of the images. In contrast, when photographs are taken in controlled indoor environments, these external factors are minimized, leading to differences in the SSIM values between indoor and outdoor test conditions.

Furthermore, the Gaussian filter's ability to reduce high-frequency noise while preserving image structure might explain why it performs slightly better than the Median filter. The Median filter tends to blur edges more severely, leading to reduced structural similarity.

In this discussion, the study cannot directly compare SSIM values with previous works due to differences in experimental methods. The study by [23] reported SSIM values of 0.44 and 0.41 for two datasets captured by drones at a maximum altitude of 140 meters. However, it does not provide detailed SSIM readings at various altitude levels. Other studies, such as that Tian et al. [12], utilized signal-to-noise ratio (SNR) measurements at different drone heights, while Lim et al. [13] used NIIRS to assess the clarity of drone images. In contrast, this work focuses on SSIM as a metric for image quality, as it better aligns with human perception compared to other metrics. Additionally, this study differs from most previous research, which has concentrated on outdoor scenarios and high-altitude drone flights. The current experiment involves controlled indoor tests and evaluates the impact of noise-reduction filters on SSIM. This layered analysis offers a more practical framework for field deployment, particularly for near-ground inspections, such as analyzing PV panels.

This study is limited to image captures between 0.7m and 2.5m, and therefore may not generalize to high-altitude drone operations. Only one drone model, which is the DJI Air 2S and a single type of solar panel were tested. Environmental factors such as extreme weather, terrain variation, or seasonal changes were not fully addressed. Also, SSIM alone was used as the quality metric; a more robust evaluation could include PSNR, NIIRS, or FSIM.

4. Conclusion

The experiments conducted in this study demonstrate that the drone's height during image capture significantly impacts image quality. Though the time of day (morning vs. evening) has a minimal effect, environmental conditions such as rain and wet surfaces notably diminish image quality. According to the study's findings, the optimal height of 1.0m should be emphasized for drone-based image-capturing applications such as solar panel inspection, surveillance, and agriculture, particularly where image quality is crucial. The findings show that, at 1.0 m, indoor and outdoor image quality, as determined by SSIM, is consistently greater, with little change due to outside influences like wind or lighting. This means that this altitude is excellent for low-altitude image-based jobs since drones operating at this level can acquire more accurate and dependable visual data. For future work, experiments should be conducted in actual PV farms to validate findings and understand real-world conditions. Investigating diverse environmental factors, optimizing drone paths and speeds, and employing advanced image processing techniques could improve image quality. Developing automated systems for real-time quality assessment and evaluating different drone models and camera systems will enhance the reliability of drone-based image assessments. Additionally, conducting long-term studies on seasonal variations and establishing standard protocols for operators will ensure consistent and optimal image capture practices. Addressing these recommendations will improve outcomes for applications like PV farm monitoring and maintenance.

Acknowledgement

We are deeply grateful to all those who played a role in the success of this project. Thank you to the College of Engineering and Research Management Centre (RMC), Universiti Teknologi MARA. This research was funded by Universiti Teknologi MARA under Grant No. 600-RMC 5/3/GPM (022/2022).

Conflict of Interest

Authors declare that there is no conflict of interests regarding the publication of the paper.

Author Contribution

The authors confirm contribution to the paper as follows: ***Conceptualization, methodology, writing, and project administration:*** *Suhaili Beeran Kutty;* ***data collection:*** *Muhammad Nuh Shamsudin, Asyraf Ahmad Safri, Mohamad Ad-Fadhil Musa****; analysis and interpretation of results:*** *Muhammad Nuh Shamsudin, Suhaili Beeran Kutty;* ***review, editing, and proofreading:*** *Puteri Nor Ashikin Megat Yunus. All authors reviewed the results and approved the final version of the manuscript.*

References

[1] Li, Q., Zhang, Z., Sun, C., Lv, X., Lian, Y., & Xing, J. (2021). An adaptive unsupervised method for powerline aerial image quality assessment. In *2021 IEEE 3rd International Conference on Power Data Science (ICPDS)* (pp. 57-61). https://doi.org/10.1109/ICPDS54746.2021.9689932

[2] Al Najjar, Y. (2022). Comparative analysis of image quality assessment metrics: MSE, PSNR, SSIM and fsim. *International Journal of Science and Research (IJSR)*, 13(3). https://doi.org/10.21275/sr24302013533

[3] Sara, U., Akter, M., & Uddin, M. S. (2019). Image quality assessment through FSIM, SSIM, MSE and PSNR—a comparative study. *Journal of Computer and Communications*, 7(3), 8-18. https://doi.org/10.4236/jcc.2019.73002

[4] Chebbi, E., Benzarti, F., & Amiri, H. (2014). An improvement of structural similarity index for image quality assessment. *Journal of Computer Science*, 10(2), 353-360. https://doi.org/10.3844/jcssp.2014.353.360

[5] Al-Wathinani, A. M., Alhallaf, M. A., Borowska-Stefańska, M., Wiśniewski, S., Sultan, M. A. S., Samman, O. Y., Alobaid, A. M., Althunayyan, S. M., & Goniewicz, K. (2023). Elevating healthcare: Rapid literature review on drone applications for streamlining disaster management and prehospital care in saudi arabia. *Healthcare*, 11(11), 1575. https://www.mdpi.com/2227-9032/11/11/1575

[6] Singh, A., Chougule, A., Narang, P., Chamola, V., & Yu, F. R. (2022). Low-light image enhancement for uavs with multi-feature fusion deep neural networks. *IEEE Geoscience and Remote Sensing Letters*, 19, 1-5. https://doi.org/10.1109/LGRS.2022.3181106

[7] Priyanka, G., Choudhary, S., Anbazhagan, K., Naresh, D., Baddam, R., Jarolimek, J., Parnandi, Y., Rajalakshmi, P., & Kholova, J. (2023). A step towards inter-operable unmanned aerial vehicles (uav) based phenotyping; a case study demonstrating a rapid, quantitative approach to standardize image acquisition and check quality of acquired images. *ISPRS Open Journal of Photogrammetry and Remote Sensing*, 9, 100042. https://doi.org/https://doi.org/10.1016/j.ophoto.2023.100042

[8] Chehri, A., Jeon, G., Fofana, I., Imran, A., & Saadane, R. (2021). Accelerating power grid monitoring with flying robots and artificial intelligence. *IEEE Communications Standards Magazine*, 5(4), 48-54. https://doi.org/10.1109/MCOMSTD.0001.2000080

[9] Rozi, M. W. F. M., & Shahbudin, S. (2023, 15-16 Aug. 2023). Photovoltaic module defects classification analysis using shufflenet architecture in electroluminescence images. In *2023 9th International Conference on Computer and Communication Engineering (ICCCE)* (pp. 294-298). https://doi.org/10.1109/ICCCE58854.2023.10246047

[10] Benatto, G. A. d. R., Mantel, C., Spataru, S., Lancia, A. A. S., Riedel, N., Thorsteinsson, S., Poulsen, P. B., Parikh, H., Forchhammer, S., & Sera, D. (2020). Drone-based daylight electroluminescence imaging of pv modules. *IEEE Journal of Photovoltaics*, 10(3), 872-877. https://doi.org/10.1109/JPHOTOV.2020.2978068

[11] Høiaas, I., Grujic, K., Imenes, A. G., Burud, I., Olsen, E., & Belbachir, N. (2022). Inspection and condition monitoring of large-scale photovoltaic power plants: A review of imaging technologies. *Renewable and Sustainable Energy Reviews*, 161, 112353. https://doi.org/https://doi.org/10.1016/j.rser.2022.112353

[12] Tian, W., Kan, Z., Sanchez-Azofeifa, A., Zhao, Q., & He, G. (2024). Image quality assessment of uav hyperspectral images using radiant, spatial, and spectral features based on fuzzy comprehensive evaluation method. *IEEE Geoscience and Remote Sensing Letters*, 21, 1-5. https://doi.org/10.1109/LGRS.2024.3353706

[13] Lim, P. C., Kim, T., Na, S. I., Lee, K. D., Ahn, H. Y., & Hong, J. (2018). Analysis of uav image quality using edge analysis. *International Archives of the Photogrammetry, Remote Sensing and Spatial Information Sciences*, XLII-4, 359-364. https://doi.org/10.5194/isprs-archives-XLII-4-359-2018

[14] Kaamin, M., Azmidi, M. I., Faisal, M. H. A., Zaini, N. Z., Sahat, S., Nor, A. H. M., Mokhtar, M., Ahmad, N. F. A., & Kamal, M. A. M. (2023). Production and evaluation of orthophoto map using uav photogrammetry. *Journal of Advanced Research in Applied Sciences and Engineering Technology*, 33(1), 187-196. https://doi.org/10.30564/jees.v6i2.6360

[15] Dąbrowski, R., & Jenerowicz, A. (2015). Portable imagery quality assessment test field for uav sensors. *Int. Arch. Photogramm. Remote Sens. Spatial Inf. Sci.*, XL-1/W4, 117-122. https://doi.org/10.5194/isprsarchives-XL-1-W4-117-2015

[16] Benjak, J., & Hofman, D. (2022). 4k video coding efficiency in uav systems. In *2022 45th Jubilee International Convention on Information, Communication and Electronic Technology (MIPRO)* (pp. 470-475). https://doi.org/10.23919/MIPRO55190.2022.9803366

[17] Segovia Ramírez, I., Pliego Marugán, A., & García Márquez, F. P. (2022). A novel approach to optimize the positioning and measurement parameters in photovoltaic aerial inspections. *Renewable Energy*, 187, 371-389. https://doi.org/https://doi.org/10.1016/j.renene.2022.01.071

[18] Köntges, M., Morlier, A., Eder, G., Fleiß, E., Kubicek, B., & Lin, J. (2020). Review: Ultraviolet fluorescence as assessment tool for photovoltaic modules. *IEEE Journal of Photovoltaics*, 10(2), 616-633. https://doi.org/10.1109/JPHOTOV.2019.2961781

[19] Desai, B., Kushwaha, U., & Jha, S. (2020). Image filtering - techniques, algorithm and applications. *GIS Science Journal*, 7(11), 970-975. https://drive.google.com/file/d/1OXE4GL3XxysPq83h9KX5gOMeFFwD0RLU/view

[20] Uhrina, M., Hlubik, J., & Vaculik, M. (2012). Correlation between objective and subjective methods used for video quality evaluation. In *2012 ELEKTRO* (pp. 103-108). https://doi.org/10.1109/ELEKTRO.2012.6225581

[21] Bakurov, I., Buzzelli, M., Schettini, R., Castelli, M., & Vanneschi, L. (2022). Structural similarity index (ssim) revisited: A data-driven approach. *Expert Systems with Applications*, 189, 116087. https://doi.org/https://doi.org/10.1016/j.eswa.2021.116087

[22] Bian, T. (2020). An ensemble image quality assessment algorithm based on deep feature clustering. *Signal Processing: Image Communication*, 81, 115703. https://doi.org/https://doi.org/10.1016/j.image.2019.115703

[23] Toki, S. A., Slack, S. G., & Coopmans, C. (2024). Image quality assessment of uav simulator imagery based on different orthomosaic maps. *2024 International Conference on Unmanned Aircraft Systems*, 923–928. https://doi.org/10.1109/ICUAS60882.2024.10556972